J | P | S | T

http://jpst.irost.ir

Journal of Particle Science and Technology

IROST

Evaluation of breakage and coalescence kernel constants for a mixer tank in the copper solvent extraction unit

Soroush Parvizi*[,1], Sirvan Aosati[2], Eskandar Keshavarz Alamdari[2], Seyed Hassan Hashemabadi[3]

[1] *Department of Materials Engineering, Shahid Rajaee Teacher Training University (SRTTU), Tehran, Iran*

[2] *Department of Materials and Metallurgical Engineering, Amirkabir University of Technology (AUT), Tehran, Iran*

[3] *School of Chemical Engineering, Iran University of Science and Technology (IUST), Tehran, Iran*

HIGHLIGHTS

- New breakage and coalescence equation constants have been developed.
- Very well agreement with available experimental data has been found.
- Parametric study of the kernels in different conditions and designs has been done.
- A simplified PBM has been derived for CFD simulation.

GRAPHICAL ABSTRACT

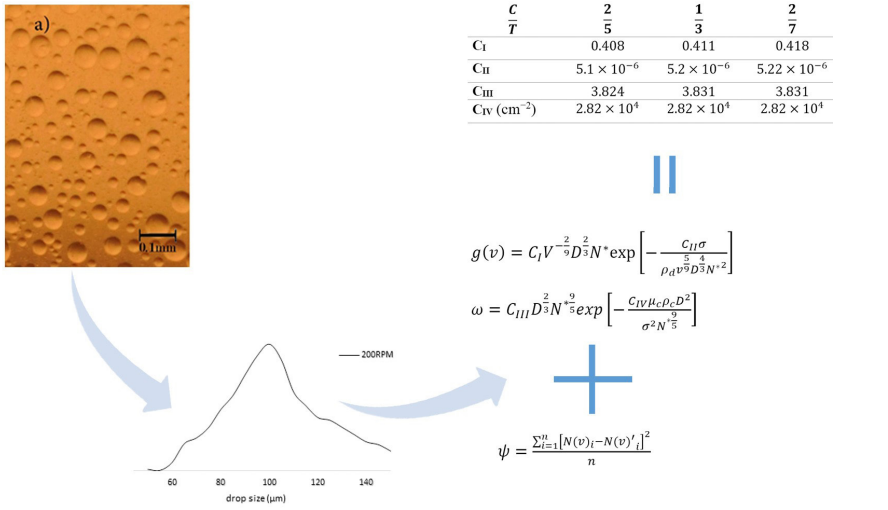

$\frac{C}{T}$	$\frac{2}{5}$	$\frac{1}{3}$	$\frac{2}{7}$
C_I	0.408	0.411	0.418
C_{II}	5.1×10^{-6}	5.2×10^{-6}	5.22×10^{-6}
C_{III}	3.824	3.831	3.831
C_{IV} (cm^{-2})	2.82×10^4	2.82×10^4	2.82×10^4

ARTICLE INFO

Article history:

Received 17 November 2019
Revised 20 June 2020
Accepted 22 June 2020

Keywords:

Coalescence kernel
Breakage kernel
Computational fluid dynamics
Solvent extraction
Copper

ABSTRACT

Since the Population Balance Model (PBM) poses a significant problem (due to the effect of droplets size distribution on the mass transfer phenomenon) in mixers, researchers face difficulties during a Population Balance Equation (PBE) numerical investigation. Therefore, investigating PBM in mixers became more considerate in recent researches. In this study, the droplet size distribution of the organic phase, which is discrete in the aqueous phase, was obtained using experimental methods and experimental data analysis. A variance function, which produces different values between PBEs and experimental data, was used to obtain the constants of breakage and coalescence kernels. Results showed that the impeller speed and clearance had no effect on the PBEs constants. In addition to these operation parameters, impeller diameter and baffle width had very little effect on these constants. In contrast, the impeller type and the number of baffles had a large specific effect on the contents by deformation of the vortex configurations.

* *Corresponding author: Tel.: +9821-22970060 ; Fax: +9821-22970033 ; E-mail address: parvizi@sru.ac.ir ; soroush.parvizi@aut.ac.ir*

DOI: 10.22104/jpst.2020.3924.1161

1. Introduction

Optimization of industrial processes with sufficient accuracy, the least cost, and in the minimum possible time is inevitably an essential matter for industry. The solvent extraction process is an essential part of hydrometallurgical units, which are widely used to produce precious and strategic metals, including copper. Mixers are one of the core components in the solvent extraction process that are responsible for the proper mixing of aqueous and organic phases [1]. The dispersion of liquid-liquid is one of the most significant problems in mixers and can create significant effects on the performance by changing the chemical composition of the system [2]. Correctly developing the equilibrium of PBMs, much the same as turbulence equations, has a powerful ability to resolve issues in hydrometallurgical industries. Nowadays, most solvent extraction mixers currently in use have inferior performance. In other words, these units have some undesirable effects on industrial reactions.

A mixer-settler, where two immiscible fluids come into contact, is one of the most crucial industrial vessels in the metallurgical industry. Due to the extraordinarily hydrodynamic conditions in these tanks, an experimental design is practically unusable to study the mixer's performance. Also, there are very many limitations in empirical studies [2-4]. As a result, it is impossible to consider the safety margin, so it is necessary to carry out a considerable number of experiments. A precise understanding of the mixing process with the ability to predict the process can help to optimize the process, economics, and safety of these systems [5].

The majority of the current liquid-liquid reactors suffer from inefficient design, which results in undesirable effects on the mixer performance. Stirred vessels, rotor-stator mixers, static mixers, valve or Jet Homogenizers, and extraction columns are examples of industrial process equipment used in contact liquid-liquid systems. Due to the very complex hydrodynamic conditions prevalent in most of these commercially available contractors/reactors, designing such units is very difficult without extensive empirical study [6,7]. Stirred tanks are the most commonly used reactors in metallurgical process industries. The operating conditions and vessel geometry design, as well as the positions of the inlet and outlet stream, have an incredible effect on the mixer's performance as they determine the hydrodynamics and turbulence intensities in the vessel. Nevertheless, these reactors are faced with many drawbacks due to the uniformity, where mixing, drop size distributions, and phase ratio (hold-up) cause wide local variations and effectiveness changes [1,7].

The operating conditions in liquid-liquid mixing tanks are directly influenced by the mixer geometry, the inlet-outlet flows, and their positions, which have an effect on the hydrodynamics and turbulence of vortex in the vessels. Therefore, since the distribution of the droplets is dramatically affected by geometry, these types of reactors have many drawbacks based on different their geometries [8].

The population balance in these systems is modeled using the population equations in equilibrium models, which represent an indefinite integral equation of the density function of the number of droplets [9,10]. Breakage is related to the interaction rate between droplets, and the breakage rate is determined by the energy dissipation rate. Accordingly, the distribution of droplet size varies considerably between the distinct parts of the mixer [11,12]. Despite all of the investigations on the hydrodynamics of mixing, dispersion is still one of the most important issues in a mixing vessel. Chemical, physical, and geometrical properties affect PBEs [13].

The other part of the PBM equations is the coalescence term, and due to turbulent flow, researchers have recognized this term as a random contingent. This term is included in the assumptions made by Ross and Coulaloglou [14,15]. All subsequent research on coalescent models has followed this approach. Hence, models that are available today are typically used to check the time of interaction or discharge. Researchers such as Kamp [16] have highlighted the disadvantages of these models while formulating their models [15,17]. Bąk and Podgórska investigated the effect of impeller speed on the transient drop size distribution and breakage and coalescence kernels of a multiphase fluid batch dispersion system [18]. They analyzed the drop size distribution evolution at the same concentration and found dramatic increases in the coalescence when the impeller speed increased, and stability in the drop size distribution diagram was obtained in the shortest mixing time with higher impeller speed.

Similarly, the breakage and coalescence kernels were dependent on the position of the impeller [18]. And Raikar *et al.* studied the effect operating parameters had on the coalescence kernel and modeled the Population

Balance Model (PBM) by analyzing experimental investigation data [19]. They concluded that the drop breakage term in PBEs has enough ability to predict the drop size distributions. Also, PBEs showed some potential for guiding experimental efforts.

PBEs are widely used as a simplified tool to describe and predict dispersed phase behavior during drop breakage and coalescence processes in terms of identifiable physical parameters and operational conditions. Their ultimate success relies on the equation's ability to describe the overall drop breakage/coalescence processes. The objective of this study is to explore the possibility of using PBE as a successful model in drop breakage and coalescence processes simulation coupled with turbulently flowing liquid-liquid dispersions. Furthermore, since our desired mixer hydrodynamic conditions are closely comparable to isotropic turbulent flow, it is expected that the drop breakage/coalescence kernels obtained in this work will have enough quality and ability to predict other more complex hydrodynamic problems and reactor's simulations [7].

Analysis of both breakage and coalescence functions, and comparisons of these results is one of the most popular ways to calculate breakage/coalescence kernels and their constants [20,21]. Although there are many computing methods to obtain the kernel's constants [22], in this study, the in-place analysis was used for the experimental investigation. MATLAB was used for digital image analysis. The breakage and coalescence kernel constants were obtained by a comparison between the dispersion indexes of the experimental and CFD analysis results. In addition to digital analysis and calculations, a CFD simulation of PBM and multiphase flow was used to validate the coding and experimental results of this study.

2. Experimental Method

The experimental setup is shown in Fig. 1 includes the camera (with 1000 FPS capabilities) and two projectors (640 nm) as the image recorder set combined with the vessel, mixer, and the reflecting surface as indicated. The cross-section details of the Pyrex mixer tank are demonstrating in Fig. 2. Three types of impellers were considered in this research: RT, PTD, and PTU.

The operational parameters of the mixer in the copper solvent extraction unit were investigated in this study. Organic (Kerosene 10 $g.l^{-1}$ DEHPA) and aqueous

Fig. 1. Experimental setup: A: lighting projector, B: camera with digital system analysis, C: impeller speed controller, D: dynamic mixer, E: reflective plate, and F: mixing vessel.

(H_2SO_4 35 $g.l^{-1}$ Cu) phases were obtained from the Sarcheshmeh Copper Complex. Table 1 demonstrates the physical properties of the organic and aqueous phases. The droplet size distribution was recorded by a high frame per second camera. Adjusting the intensity of the light source increased the optical contrast in the resulting images. In addition to the control system of the light source, light filters with a wavelength of 640 nm were installed during the experimental investigation. This was necessary for imaging the moving droplets and image analysis. The resulting images were analyzed by image analysis software (MATLAB) for measuring the droplet size dispersion.

The key point is the presence of copper ions in the aqueous phase. In fact, the presence of copper ions in

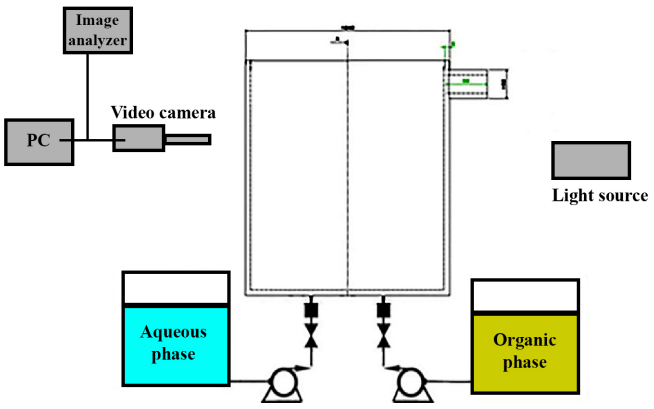

Fig. 2. Laboratory-scale of the mixer.

Table 1. Physical properties of the organic and aqueous phase at 200 °C.

Aqueous viscosity (mPa.s)	Organic viscosity (mPa.s)	Aqueous density ($kg.m^{-3}$)	Organic density ($kg.m^{-3}$)	Surface tension ($mN.m^{-1}$)
26.1	806	1100	3.3	2.3

the aqueous phase was the impacting agent for mass transfer. Impeller specifications and speeds used in experiments are shown in Table 2. Table 3 demonstrates the other experimental conditions.

3. Mathematics Theory

The two-phase Eulerian/Eulerian model was considered using the *k-ε* model for the continuous phase and PBM for the discrete phase [23,24]. Using PBM in modeling requires four constants, which were obtained and discussed in this study. In many hydro-metallurgical and solvent extraction processes, the turbulent flow affects the characteristics of the dispersed phase, such as droplets size and droplet size distribution. In this study, the geometry of the aqueous and organic phase inlets was designed according to Luo's research [24]. The linear scale of the vortex is expected to be as Eq. (1).

$$\lambda_k = (v''^3/\varepsilon)^{(1/4)} \quad (1)$$

where, ε is the energy dissipation rate and λ_k is a linear scale of the vortex. The droplets' breakage was affected by the interaction of the vortexes on the droplets; breakage occurred if the energy of this interaction was more than the surface energy resulting from droplets breakage. Additionally, coalescence occurred when two or more droplets interacted due to a sharp decrease in kinetic energy. Broadly, the process of coalescence involved three steps. As time progresses, the rate of breaking and coalescence varies, but on establishing the equilibrium, both values were relatively equal [25].

PBM equations are dynamical and include integrals with boundary conditions which have yet to have analytic solutions. Therefore, numerical methods have been developed to solve PBM equations [26]. In a cell where PBM equations rule is established, four processes can occur on the droplets (Fig. 3). These processes determine droplet size distributions. In this cell, temperature, concentration, and other internal variables represent fixed, only coalescence, and breakage occurring in the dispersed phase [27].

The equilibrium equation in the previous conditions, which receive another statement of the continuity

Table 2. Mixer specifications used in the experiments.

Specification	Value
Clearance	7 cm
Baffle width	21 mm
Number of baffles	4
Impeller type	RT
Impeller diameter	7 cm
Impeller speed	150-200-250 rpm

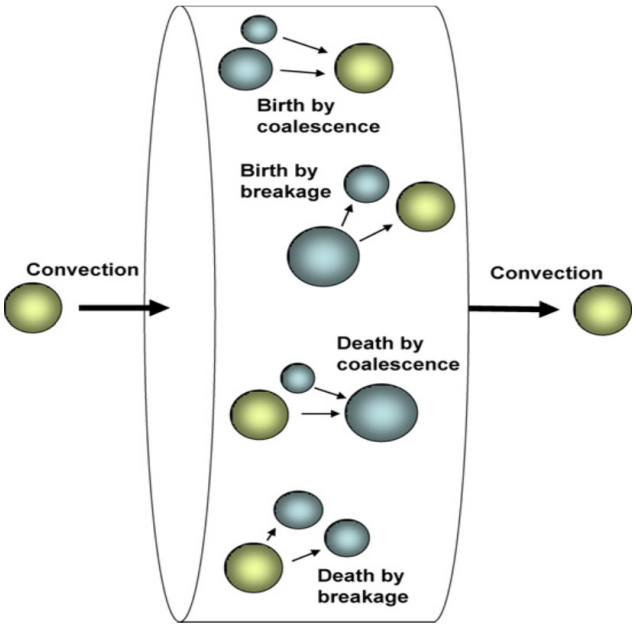

Fig. 2. Four possible processes resulted from the interaction between the droplets and vertex in the physical volume where PBM equations rule established [2].

Table 3. Other experimental conditions of the solvent extraction mixer unit.

Reynolds numbers	Dispersed phase hold-up (%)	Aqueous and organic velocity ($m.s^{-1}$)	Inter-camera spacing (mm)
21000-50000	50	0.2	50

equation, was expected to be as Eq. (2) [16, 28-35].

$$\frac{\partial}{\partial t}N + \nabla_x.\dot{X}N + \nabla_r.\dot{R}N = h \quad (2)$$

where N is the number of droplets, $\nabla_x.\dot{X}N$ is the term of the position of droplets, $\nabla_r.\dot{R}N$ is the term of the size of droplets, and h is the source term of droplets change. Eq. (2) can be expressed in the limited term of coalescence and breakage by Eq. (3).

$$\frac{\partial}{\partial t}[N(V,t)] + \nabla.[\vec{u}N(V,t)] = S(V,t) \quad (3)$$

where $\vec{u}$ is the relative velocity between two points, $N(V,t)$ is the number of droplets with V volume in time t, and $S(V,t)$ is the term of coalescence and breakage. In this study, the high-pressure mixing model, as a well-mixed multiphase system, is used to measure the initial drop distribution. Each pass corresponds to one dimensionless time unit.

$$N(V,t) = \frac{V_{tot}n_p(V,t)}{V} \quad (4)$$

Where V_{tot} conserved the total volume of the drops. In Eq. (3), $S(V,t)$ is a term of coalescence and breakage, shown in Fig. 3, and is expected to be as Eq. (5).

$$S(V,t) = B^C(V,t) - D^C(V,t) + B^C(V,t) - D^C(V,t) \quad (5)$$

where $B^C(V,t)$ and $B^C(V,t)$ are the birth rates of droplet, $D^C(V,t)$ and $D^C(V,t)$ are the death rates of droplet, by breakage and coalescence with V volume in time t.

In Eq. (5), B^b and D^b are the birth and death rates of droplet by breakage, and B^c and D^c are the birth-death rates of droplet by coalescence. Therefore, the equations are expected to be:

$$B^b = \int_{\Omega V} pg(V')\,\beta(V/V')\,n(V')\,dV' \quad (6)$$

$$D^b = g(V)\,n(V) \quad (7)$$

$$B^c = 0.5\int_0^V a(V-V',V')\,n(V-V')\,n(V')\,dV' \quad (8)$$

$$D^c = \int_0^V a(V,V')\,n(V)\,n(V')\,dV' \quad (9)$$

The PBE model contains two breakage and coalescence functions that must be specified to generate predictions. Based on other studies in this field [14,16, 27-31,36-39], mathematical equations are not available for the number of drop daughters upon breakage, and the daughter drop distribution is the same as coalescence. Although some researchers believe there are multiple breakages [14,36,40]. In this work, binary breakage ($n(V)$=2) has been used to simplify and consider the limitations. Therefore, it was assumed that $\beta(V,V')$ is created based on the normal distribution function as Eq. (10).

$$\beta(V,V') = \frac{2.4}{V'}exp\left[-4.5\frac{(2V-V')^2}{(V')^2}\right] \quad (10)$$

The consideration focuses on the breakage rate as a two-term equation that explicitly depends on the physical properties [19]. Although unlike the general breakage functions, we did not consider this term of PBEs as a unique function, which accounts for the small effect of the dispersed phase viscosity; nonetheless, it is clear that the breakage time (t_B) is assumed to be dependent on drop volume.

$$t_B = K_I V^{\frac{2}{9}}\left(\frac{\varepsilon}{\rho_d}\right)^{-\frac{1}{3}} \quad (11)$$

The breakage function was specialized to high-pressure mixers by using the following relation between the energy dissipation rate and the pressure P.

$$\varepsilon = K_{II}P^{\frac{3}{2}}V^{-\frac{1}{3}}\rho_d^{-\frac{3}{2}} \quad (12)$$

However, breakage and coalescence models are a mixture of a probability of interaction (between the droplet and turbulent flow) with enough energy. Coulaloglou *et al.* [15] suggested assumptions for the energy distribution and the diameter of the droplets that will simplify the equations. As mentioned above, the breakage and coalescence frequency is expected to be as Eqs. (13) and (14) [14,15,40].

$$g(v) = C_I V^{-\frac{2}{9}}D^{\frac{2}{3}}N^*\exp\left[-\frac{C_{II}\sigma}{\rho_d v^{\frac{5}{9}}D^{\frac{4}{3}}N^{*2}}\right] \quad (13)$$

$$\omega = C_{III}D^{\frac{2}{3}}N^{*\frac{9}{5}}exp\left[-\frac{C_{IV}\mu_c\rho_c D^2}{\sigma^2 N^{*\frac{9}{5}}}\right] \quad (14)$$

where K_I and K_{II} are parameters determined from obtained drop size distributions. Note that the breakage rate of the dispersed phase density ρ_d, impeller speed N^*, impeller diameter D, continues phase viscosity

μ_c, and the interfacial tension σ of C_I - C_{IV} in the frequency functions of the coalescence and breakage are adjustable. Thereafter, the optimal values of the function constants are obtained by minimizing the variation between the predict function and experimental results (the experimental results include the droplet size distribution). In this study, the variance (ψ) was used to calculate the variation as shown in Eq. (15)[19].

$$\psi = \frac{\sum_{i=1}^{n}\left[N(v)_i - N(v)'_i\right]^2}{n} \quad (15)$$

Here, $N(v)'_i$ is the droplet size distribution of droplets with volume V_i, $N(v)_i$ is the predicted value, and n is the number of the total intervals for the size of the droplets. There are constant values dependent on the physical properties of the system in the breakage and coalescence frequency equations, which were computed according to Table 4.

4. Results and discussion

4.1. Experimental determination of liquid-iquid contact

Fig. 4 compares the experimental investigation results of the droplet size distribution at different impeller speeds. It is clear that impeller speed has a major effect on the droplet parameter in the mixer unit due to the increase in the number of the droplets and the decrease in the droplet size. Moreover, increasing the impeller speed from 150 to 250 rpm has little effect on droplet properties and the mixing volume. The size of the vortexes was the reason for this behavior. When the impeller speed was less than 250 rpm, the entire effective volume of the mixer was not involved in the mixing process; also, the vortex size was not large enough to affect all the fluid in the unit [1,41]. Most of the energy added to increase the impeller speed from 250 to 300 rpm was spent to change the breakage and coalescence kernels.

Table 4. Constant values in the equations of breakage and coalescence rates.

Parameter	Unit	Value
σ	N.m^{-1}	0.0261
N^* (impeller speed)	rpm	200
ρ_d	kg.m^{-3}	806
ρ_c	kg.m^{-3}	1100
μ_c	mPa.s	2.3

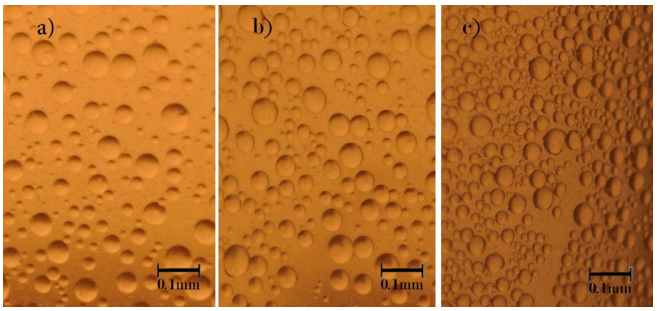

Fig. 4. Image of droplets at different impeller speeds: a) 150, b) 250, and c) 300 rpm.

4.2. Computation of coalescence and breakage kernel constants

The droplet size distribution in the mixer, which was obtained from analyzing experimental data by image processing and mathematical solution, is shown in Figs. 5-7. The results obtained for these constants are shown in Table 5.

It is evident that the maximum droplet size decreased, and the droplet distribution became more restrictive with increased impeller velocity (Fig. 5). On the other hand, the impeller speed influenced the intensity of the turbulent flow. Also, more separation occurred in the mixer tank as the impeller speed increased due to centrifugal forces. However, the breakage and coalescence kernel also increased because of higher impeller speed; hence both functions changed on the different positions. So, the breakage kernel increased more than the coalescence kernel in all vessel volumes at increased impeller speed.

According to Fig. 6, the droplet size distribution does not change significantly by amending the clearance, and changes were not significant in the other sections of this diagram. This means the impeller position had no effect

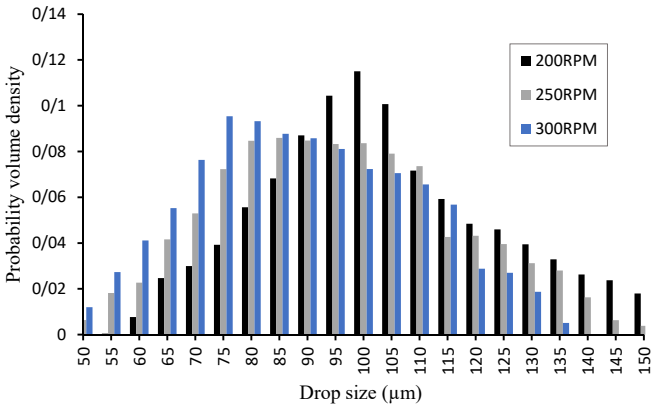

Fig. 5. Effect of impeller speed on droplet size distribution.

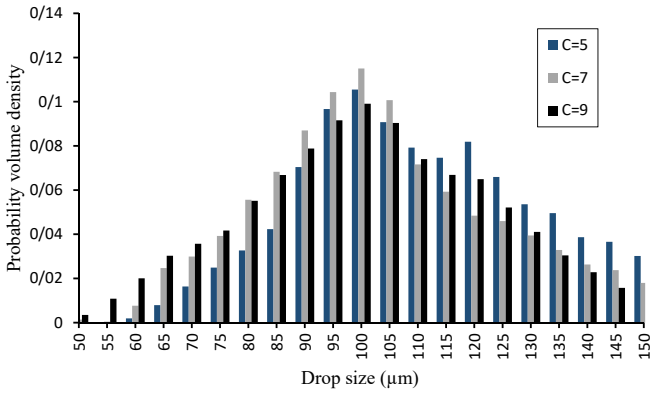

Fig. 6. Effect of clearance on droplet size distribution.

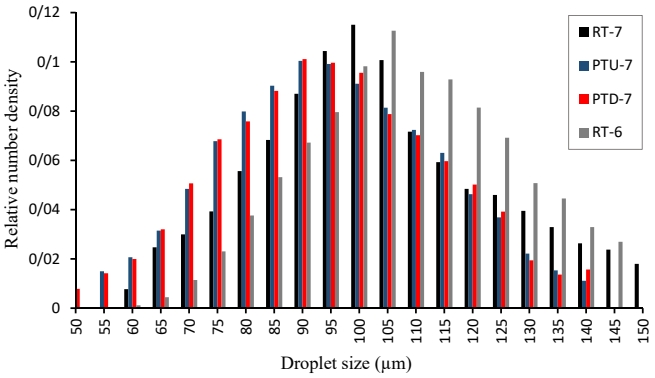

Fig. 7. Effects of impeller type and diameter on droplet size distribution.

on the breakage and coalescence kernels. Also, the PTD and PTU impellers produced approximately similar conditions in terms of the droplet size distribution, in contrast to Rewatkar and Joshi [32], who showed that the PTD impeller had more energy efficiency than the PTU impeller (Fig. 7). Furthermore, the size of the droplets decreased at the higher impeller diameter. Conversely, the produced vortex configure by RT was different than PTD and PTU due to the rate of the breakage and coalescence kernels.

The (lowest) effect of impeller speed and clearance on C_I - C_{IV} (Tables 5 and 6) is clear based on comparable results. The geometry design creates the least changes. Therefore, these operation parameters had no effect on breakage and coalescence kernel constants. Therefore, the changes in Tables 5 and 6 can be ignored during the next analysis steps.

Even small changes in the mixer geometry can modify breakage and coalescence kernels. Tables 7 and 8 demonstrate the modification effect in terms of the PBEs constants. Also, these tables represent the effect of vortex properties (configuration in general) on PBEs. Based on other studies, the geometry design is the only source for breakage and coalescence constants change. These constants are a function of the vortex configuration and the geometrical changes of the vessel. Tables 7 and 8 prove that any changes in mixing geometry quickly show themselves on the kernels and constants.

Table 5. Effect of impeller speed on C_I - C_{IV}, obtained from the analysis of experimental data.

Impeller speed (rpm)	**200**	**250**	**300**
C_I	0.411	0.415	0.417
C_{II}	5.2×10^{-6}	5.2×10^{-6}	5.2×10^{-6}
C_{III}	3.831	3.835	3.826
C_{IV} (cm^{-2})	2.82×10^{4}	2.82×10^{4}	2.82×10^{4}

Table 6. Effect of clearance on C_I - C_{IV}, obtained from the analysis of experimental data.

$\frac{C}{T}$	$\frac{2}{5}$	$\frac{1}{3}$	$\frac{2}{7}$
C_I	0.408	0.411	0.418
C_{II}	5.1×10^{-6}	5.2×10^{-6}	5.22×10^{-6}
C_{III}	3.824	3.831	3.831
C_{IV} (cm^{-2})	2.82×10^{4}	2.82×10^{4}	2.82×10^{4}

The effect of the impeller type and the number of baffles on C_I - C_{IV} constants was predictable. These constants were only affected by the mixer design (Tables 9 and 10). In particular, the vortex configuration and size affect the constants of breakage and coalescence.

Table 7. Effect of impeller diameter on C_I - C_{IV}, obtained from the analysis of experimental data.

$\frac{D'}{T}$	$\frac{2}{5}$	$\frac{1}{3}$	$\frac{2}{7}$
C_I	0.495	0.411	0.341
C_{II}	5.1×10^{-6}	5.2×10^{-6}	5.3×10^{-6}
C_{III}	3.712	3.831	3.95
C_{IV} (cm^{-2})	2.80×10^{4}	2.82×10^{4}	2.87×10^{4}

Table 8. Effect of baffle width on C_I - C_{IV}, obtained from the analysis of experimental data.

$\frac{b}{T}$	**0.1**	**0.125**	**0.15**
C_I	0.411	0.455	0.484
C_{II}	5.2×10^{-6}	4.31×10^{-6}	3.12×10^{-6}
C_{III}	3.712	3.831	3.95
C_{IV} (cm^{-2})	2.82×10^{4}	2.80×10^{4}	2.74×10^{4}

Table 9. Effect of impeller type on C_I - C_{IV}, obtained from the analysis of experimental data.

Impeller type	PTD	RT	PTU
C_I	0.58	0.411	0.576
C_{II}	2.18×10^{-6}	5.2×10^{-6}	2.18×10^{-6}
C_{III}	3.168	3.831	3.18
C_{IV} (cm^{-2})	2.46×10^{4}	2.82×10^{4}	2.46×10^{4}

Table 10. Effect of the number of the baffle on C_I - C_{IV}, obtained from the analysis of experimental data.

n_b	3	4	6
C_I	0.394	0.411	0.488
C_{II}	5.2×10^{-6}	5.2×10^{-6}	3.80×10^{-6}
C_{III}	3.746	3.831	3.974
C_{IV} (cm^{-2})	2.82×10^{4}	2.82×10^{4}	2.78×10^{4}

As mentioned above, the impeller speed and clearance did not affect the breakage and breakage constants, and the impeller diameter and baffle width contribute to the low efficiency.

4.3. Computer simulation

The calculated constants in Table 5 were obtained from the physical performance properties of the system. However, according to the operating and mixer design parameters, changes were seen in the PBE constants due to turbulence flows variations, and these changes affected the turbulent flow size. The investigation results are presented in a separate article by the authors.

These values were considered universal. Therefore, they were kept unchanged at an impeller speed of 200 rpm throughout the investigation. However, the quantity of the constants found was different than those obtained by other researchers using similar methods to predict liquid-liquid dispersions [2]. Table 11 compares various researchers' results. The differences in Table 11 are due to the mathematical simplification used in this study.

Using a computer simulation of PBM using Coulaloglou's constants [36], and this study's constants data were compared to clarify the differences between the constants of this study and Coulaloglou's ones. It is important to couple PBM with the governing equations of fluid flow due to the effect of multiphase flow equations on the simulation methods. That is one of the most popular references used for the computer simulation of mixer vessels.

Table 11. Numerical values of the empirical constants calculated in other studies [2].

Proposed by	C_I	C_{II}	C_{III}	C_{IV} (m^{-2})
Coulaloglou [36]	0.00487	0.0552	2.17×10^{-4}	2.28×10^{13}
Ross *et al.* [14]	0.00487	0.08	2.17×10^{-4}	3×10^{12}
Hsia [37]	0.01031	0.06354	4.5×10^{-4}	1.891×10^{13}
Tavlarides [38]	0.00487	0.08	1.9×10^{-3}	2×10^{12}
Ribeiro *et al.* [39]	0.00481	0.0558	1.65×10^{-3}	4.74×10^{12}
This study	0.411	5.2×10^{-6}	3.831	2.82×10^{8}

Fig. 8 compares the droplet size distribution against the experimentally determined values. There is a clear discrepancy between the two simulation results. The constants obtained in this study predict the experimental results very well.

The ψ, in Eq. (15), criterion was used to calculate the matching of the simulation and experimental results. To remove the dimension, the dispersion index used as follows.

$$S=\frac{\frac{\sum_{i=1}^{n}\left|N(v)_i-N(v)'_i\right|}{n}}{\frac{\sum_{i=1}^{n}N(v)'_i}{n}}=\frac{\sum_{i=1}^{n}\left|N(v)_i-N(v)'_i\right|}{\sum_{i=1}^{n}N(v)'_i} \quad (16)$$

In the case of full accommodation, the index of dispersion from the target function tends to zero. From the simulation of the population balance at 200 rpm with PBM of the breakage and coalescence kernel obtained in this study, the dispersion index was calculated from the target function of 0.00235.

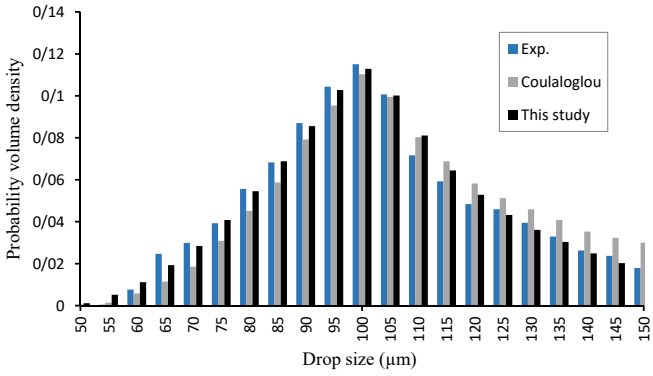

Fig. 8. Comparison between Coulaloglou [36] and this study breakage and coalescence constants.

5. Conclusion

From the findings of this study, we concluded that the droplets dispersion inside a copper solvent extraction mixer could be more accurately predicted, compared to other researcher's data, such as Coulaloglou. In this study, the stability of population balance equations was used to improve the simulation of the aqueous and organic phase in high precision hydrometallurgy in a solvent extraction mixer. The droplet size distribution inside the copper solvent extraction mixer compared with the experimental results measured with photography and image analysis techniques showed good agreement.

The obtained PBE constants provide a necessary step in the process of mixer design and improving computer simulation. Drop breakage and coalescence kernels are completely connected with tank design and process operation. Therefore, the PBE model has the potential to produce high-quality results in the drop size distribution, even when the parameters were changing.

Acknowledgments

The authors would like to acknowledge the Hydrometallurgy Research Center of the Sarcheshmeh Copper Complex, National Iranian Copper Industries Co.

Abbreviations

$a(V,V')$: Function of probability
b: Width of baffles
B^b and $B^B(V,t)$: Birth rate by breakage with V volume in time t
B^c and $B^C(V,t)$: Birth rate by coalescence with V volume in time t
C: Clearance
C_I,C_{II},C_{III} and C_{IV}: Breakage and coalescence contents
D: Droplet diameter
D': Impeller diameter
D^b and $D^B(V,t)$: Death rate by breakage with V volume in time t
D^c and $D^C(V,t)$: Death rate by coalescence V volume in time t
FPS: Frame per second
$g(V)$: Breakage frequency by V volume
$g(V')$: Coalescence frequency of droplet by V' volume
$h=S(V,t)$: Source term of equilibrium equation coalescence kernel constants
N: Number of droplets
$N(V,t)$: Number of droplets with V volume in time t
$N(v)_i$: Number of droplets (Numerical)
$N(v)'_i$: Number of droplets (Experimental)
N^*: Impeller speed
n: Number of bin
n_b: Number of baffles
nm: Nanometer
$n(V')$: Number of droplets by V' volume
$n(V)$: Number of droplets by V volume
$\vec{u}$: Relative velocity between two points
PBE: Population balance equation
PBM: Population balance model
PTD: Down flow turbine impeller
PTU: Up flow turbine impeller
RT: Rushton turbine impeller
T: Tank diameter
V'': Volume of the vessel

Greek letters

$\beta(v',v)$: Function of probability
ε: Energy dissipation rate
λ_k: Linear scale of vortex
ρ: Phase density
ρ_c: Continuous phase density
ρ_d: Disperse phase density
σ: Surface stress
μ_c: Continuous phase viscosity
v: Droplet initial volume
v': Droplet final volume
ω: Coalescence frequency
ψ: Variance

References

[1] S. Parvizi, E. Keshavarz Alamdari, S.H. Hashemabadi, S. Aosati, CFD simulation and experimental study of impeller speed and cearance effects in the mixer of copper solvent extraction unit, Indian J. Sci. Technol. 9(S1) (2016) DOI: 10.17485/ijst/2016/v9iS1/99815.

[2] F. Azizi, A. Al-Taweel, Turbulently flowing liquid-liquid dispersions. Part I: drop breakage and coalescence, Chem. Eng. J. 166 (2011) 715-725.

[3] A.W. Mahoney, D. Ramkrishna, Efficient solution of

population balance equations with discontinuities by finite elements, Chem. Eng. Sci. 57 (2002) 1107-1119.

[4] D. Ramkrishna, A.W. Mahoney, Population balance modeling. Promise for the future, Chem. Eng. Sci. 57 (2002) 595-606.

[5] M.M. Attarakih, H.J. Bart, N.M. Faqir, Numerical solution of the spatially distributed population balance equation describing the hydrodynamics of interacting liquid–liquid dispersions, Chem. Eng. Sci. 59 (2004) 2567-2592.

[6] R. Andersson, B. Andersson, F. Chopard, T. Norén, Development of a multi-scale simulation method for design of novel multiphase reactors, Chem. Eng. Sci. 59 (2004) 4911-4917.

[7] S. Parvizi, E. Keshavarz Alamdari, S.H. Hashemabadi, M. Kavousi, A. Sattari, Investigating factors affecting on the efficiency of dynamic mixers, Min. Proc. Ext. Met. Rev. 37 (2016) 342-368.

[8] F. Azizi, A. Al-Taweel, Algorithm for the accurate numerical solution of PBE for drop breakup and coalescence under high shear rates, Chem. Eng. Sci. 65 (2010) 6112-6127.

[9] E. Madadi-Kandjani, A. Passalacqua, An extended quadrature-based moment method with log-normal kernel density functions, Chem. Eng. Sci. 131 (2015) 323-339.

[10] A. Passalacqua, F. Laurent, E. Madadi-Kandjani, J.C. Heylmun, R.O. Fox, An open-source quadrature-based population balance solver for OpenFOAM, Chem. Eng. Sci. 176 (2018) 306-318.

[11] G.H. Yeoh, C.P. Cheung, J. Tu, Multiphase flow analysis using population balance modeling: Bubbles, drops and particles, Butterworth-Heinemann, Oxford, 2014.

[12] G. Narsimhan, J. Gupta, D. Ramkrishna, A model for transitional breakage probability of droplets in agitated lean liquid-liquid dispersions, Chem. Eng. Sci. 34 (1979) 257-265.

[13] E.L. Paul, V.A. Atiemo-Obeng, S.M. Kresta, Handbook of industrial mixing: Science and practice, John Wiley & Sons, NJ, 2004.

[14] S.L. Ross, F.H. Verhoff, R.L. Curl, Droplet breakage and coalescence processes in an agitated dispersion. 2: Measurement and interpretation of mixing experiments, Ind. Eng. Chem. Fund. 17 (1978) 101-108.

[15] C. Coulaloglou, L. Tavlarides, Drop size distributions and coalescence frequencies of liquid-liquid dispersions in flow vessels, AIChE J. 22 (1976) 289-297.

[16] J. Kamp, M. Kraume, Influence of drop size and superimposed mass transfer on coalescence in liquid/liquid dispersions-test cell design for single drop investigations. Chem. Eng. Res. Des. 92 (2014) 635-643.

[17] S. Das, Development of a coalescence model due to turbulence for the population balance equation, Chem. Eng. Sci. 137 (2015) 22-30.

[18] A. Bąk, W. Podgórska, Investigation of drop breakage and coalescence in the liquid-liquid system with nonionic surfactants Tween 20 and Tween 80, Chem. Eng. Sci. 74 (2012) 181-191.

[19] N.B. Raikar, S.R. Bhatia, M.F. Malone, M.A. Henson, Experimental studies and population balance equation models for breakage prediction of emulsion drop size distributions, Chem. Eng. Sci. 64 (2009) 2433-2447.

[20] N. Metta, M. Ierapetritou, R. Ramachandran, A multiscale DEM-PBM approach for a continuous comilling process using a mechanistically developed breakage kernel, Chem. Eng. Sci. 178 (2018) 211-221.

[21] F. Xiao, H. Xu, X.Y. Li, D. Wang, Modeling particle-size distribution dynamics in a shear-induced breakage process with an improved breakage kernel: Importance of the internal bonds, Colloid. Surface. A, 468 (2015) 87-94.

[22] A. Falola, A. Borissova, X.Z. Wang, Extended method of moment for general population balance models including size dependent growth rate, aggregation and breakage kernels, Comput. Chem. Eng. 56 (2013) 1-11.

[23] M. Mirzaie, A. Sarrafi, H.H. Pour, A. Baghaie, M. Molaeinasab, Experimental investigation and CFD modeling of hydrodynamic parameters in a pulsed packed column, Solvent Extr. Ion Exc. 34 (2016) 643-660.

[24] H. Luo, H.F. Svendsen, Theoretical model for drop and bubble breakup in turbulent dispersions, AIChE J. 42 (1996) 1225-1233.

[25] L.E. Patruno, C.A. Dorao, P.M. Dupuy, H.F. Svendsen, H.A. Jakobsen, Identification of droplet breakage kernel for population balance modelling, Chem. Eng. Sci. 64 (2009) 638-645.

[26] R. Xie, J. Li, Y. Jin, D. Zou, M. Chen, Simulation of drop breakage in liquid-liquid system by coupling

of CFD and PBM: Comparison of breakage kernels and effects of agitator configurations, Chinese J. Chem. Eng. 27 (2019) 1001-1014.

[27] P.J. Becker, F. Puel, H.A. Jakobsen, N. Sheibat-Othman, Development of an improved breakage kernel for high dispersed viscosity phase emulsification, Chem. Eng. Sci. 109 (2014) 326-338.

[28] M.E. Gheshlaghi, A.S. Goharrizi, A.A. Shahrivar, H. Abdollahi, Modeling industrial thickener using computational fluid dynamics (CFD), a case study: Tailing thickener in the Sarcheshmeh copper mine, Int. J. Min. Sci. Technol. 23 (2013) 885-892.

[29] N. Yang, Q. Xiao, A mesoscale approach for population balance modeling of bubble size distribution in bubble column reactors, Chem. Eng. Sci. 170 (2017) 241-250.

[30] J. Kamp, M. Kraume, Coalescence efficiency model including electrostatic interactions in liquid/liquid dispersions, Chem. Eng. Sci. 126 (2015) 132-142.

[31] M. Mirzaie, A. Sarrafi, H. Hashemipour, A. Baghaie, M. Molaeinasab, CFD simulation and experimental investigation of the copper solvent extraction in a pilot plant pulsed packed column in Sarcheshmeh Copper Complex, Heat Mass Transfer, 53 (2017) 1995-2008.

[32] V. Rewatkar, J. Joshi, Effect of impeller design on liquid phase mixing in mechanically agitated reactors, Chem. Eng. Commun. 102 (1991) 1-33.

[33] F. Lehr, D. Mewes, A transport equation for the interfacial area density applied to bubble columns. Chem. Eng. Sci. 56 (2001) 1159-1166.

[34] L. Müller, A. Klar, F. Schneider, A numerical comparison of the method of moments for the population balance equation, arXiv preprint arXiv:1706.05854 (2017).

[35] L. Liu, J. Litster, Population balance modelling of granulation with a physically based coalescence kernel, Chem. Eng. Sci. 57 (2002) 2183-2191.

[36] C.A. Coulaloglou, Dispersed phase interactions in an agitated flow vessel, PhD Thesis, Illinois Institute of Technology, Chicago, IL, USA, 1975.

[37] M.A. Hsia, The modeling of liquid-liquid extraction in stirred tanks by a simulation approach, PhD Thesis, Illinois Institute of Technology, Chicago, IL, USA, 1981.

[38] P.M. Bapat, L.L. Tavlarides, Mass transfer in a liquid-liquid CFSTR, AIChE J. 31 (1985) 659-666.

[39] L.M. Ribeiro, P.F.R. Regueiras, M.M.L. Guimaraes, C.M.N. Madureira, J.J.C. Cruz-Pinto, Dynamic behaviour of liquid-liquid agitated dispersions. I: The hydrodynamics, Comput. Chem. Eng. 19 (1995) 333-343.

[40] Z. Gao, D. Li, A. Buffo, W. Podgórska, D.L. Marchisio, Simulation of droplet breakage in turbulent liquid-liquid dispersions with CFD-PBM: comparison of breakage kernels, Chem. Eng. Sci. 142 (2016) 277-288.

[41] S. Parvizi, S. Aosati, E. Keshavarz Alamdari, Experimental study of the effect of impeller geometrical parameters on fluid hydrodynamics in copper solvent extraction mixer, Int. J. Adv. Des. Manuf. Technol. 10 (2017) 21-25.